

DREAM: On hallucinations in AI-generated content for nuclear medicine imaging

Menghua Xia¹, Reimund Bayerlein^{2,3}, Yanis Chemli¹, Xiaofeng Liu¹, Jinsong Ouyang¹, Georges El Fakhri¹, Ramsey D. Badawi^{2,3}, Quanzheng Li⁴, and Chi Liu¹

¹*Department of Radiology and Biomedical Imaging, Yale University School of Medicine, New Haven, CT, USA.*

²*Department of Biomedical Engineering, University of California Davis, Sacramento, CA, USA.*

³*Department of Radiology, University of California Davis, Sacramento, CA, USA.*

⁴*Department of Radiology, Massachusetts General Hospital and Harvard Medical School, Boston, MA, USA.*

Abstract

Artificial intelligence-generated content (AIGC) has shown remarkable performance in nuclear medicine imaging (NMI), offering cost-effective software solutions for tasks such as image enhancement, motion correction, and attenuation correction. However, these advancements come with the risk of hallucinations, generating realistic yet factually incorrect content. Hallucinations can misrepresent anatomical and functional information, compromising diagnostic accuracy and clinical trust. This paper presents a comprehensive perspective of hallucination-related challenges in AIGC for NMI, introducing the DREAM report, which covers recommendations for definition, representative examples, detection and evaluation metrics, underlying causes, and mitigation strategies. This position statement paper aims to initiate a common understanding for discussions and future research toward enhancing AIGC applications in NMI, thereby supporting their safe and effective deployment in clinical practice.

Key Words: artificial intelligence-generated content (AIGC); nuclear medicine imaging (NMI); hallucination

I Introduction

Artificial intelligence-generated content (AIGC) has demonstrated significant potential in nuclear medicine imaging (NMI) over the past decade, achieving state-of-the-art performance across various tasks, based on a range of quantification metrics. Key applications include PET/SPECT image enhancement like denoising, deblurring, and partial-volume correction (1); quantitative accuracy improvements like motion correction, scatter and attenuation correction (2); cross-modality image translation such as generating PET images from CT or MRI and vice versa (3). These AI-driven solutions offer the potential to replace traditional hardware-dependent approaches with more cost-effective software alternatives, while also potentially reducing radiation exposure, easing clinical work-

loads, and optimizing imaging workflows.

NOTEWORTHY

- Hallucinations may occur across all AIGC applications in NMI.
- Within this paper, hallucinations are defined as AI-generated abnormalities or artifacts that appear visually realistic and highly plausible, yet are factually false when compared to reference scans, deviating from anatomical or functional truth.
- Recommended detection and evaluation methods include image-level comparisons, dataset-wise statistical analysis, clinical task-based assessment (by human or model observers), and automated hallucination detectors trained on annotated benchmark datasets.
- Effective hallucination mitigation requires a comprehensive and multi-perspective approach encompassing data quality, learning paradigms, and model design.
- Substantial adaptation and continued research are needed for robust detection, evaluation, and mitigation approaches tailored to AI hallucinations in NMI.

Despite these advancements, hallucinations pose significant challenges to AIGC in NMI applications where clinical decision-making demands high fidelity. Hallucinations can lead to cascading errors, including misdiagnosis, mistreatment, unnecessary interventions, medication errors, and ethical or legal concerns (4). These risks highlight the urgent need for robust hallucination detection frameworks and mitigation strategies before AIGC can be safely deployed in clinical practice.

While recent surveys (5)(6) have explored hallucinations in natural language processing (NLP), the medical imaging community still lacks a domain-specific and systematic analysis of hallucinations. To bridge this gap, this paper presents a comprehensive perspective on hallucination-related challenges in AIGC for NMI. We introduce the DREAM report, which outlines key aspects including the **d**efinition of hallucinations, **r**epresentative examples, **d**e-

For correspondence, contact Chi Liu (chi.liu@yale.edu).

This work was supported by the National Institutes of Health (NIH) under grants R01CA275188 and P41EB022544.

Manuscript word count: 5911.

Table 1: Summary of the DREAM Report.

Definition and Representative examples			
AI-generated abnormalities or artifacts that appear visually realistic and highly plausible, yet are factually false when compared to reference scans, deviating from anatomical or functional truth. Representative examples of such hallucinations in AIGC for NMI are presented in Section III.			
Detection and Evaluation			
Perspective	Potential methods		Limitations / Future work
Image-level comparison	Hallucination index; Radiomics analysis;		<ul style="list-style-type: none">• Consensus on annotation criteria;• Hallucination-specific metrics considering clinical relevance;• Inter- and intra-observer variability studies;• Hallucination detector architecture;• etc.
Dataset-wise statistical analyses	Neural hallucination precursor; No-gold-standard evaluation (NGSE);		
Clinical task assessment	Performance on tasks such as lesion segmentation and disease classification; Bounding boxes for localization, descriptive text annotations, and Likert scoring for severity and diagnostic quality;		
Automated hallucination detector	Models trained on hallucination-annotated benchmark datasets;		
Causes and Mitigation			
Perspective	Causes	Potential methods	Limitations / Future work
Data	Domain shift	Usage guidelines specifying application ranges; Improve data quality, quantity, and diversity; Domain adaptation techniques; Transfer learning; Continuous data updates; Retrieval-augmented generation (RAG);	<ul style="list-style-type: none">• Data-efficient and generalizable approaches;• RAG techniques leveraging the benchmark dataset as retrieval repositories;• Hallucination-aware mechanisms with the hallucination detector providing feedback;• etc.
	Data nondeterminism	Optimizing data acquisition; Data preprocessing and cleaning;	
	Imperfect inputs/prompts	Optimizing input instructions; Prompt engineering;	
Learning	Inherent probabilistic nature of deep learning	Feature / model averaging; User-guided interactive alignment; Fast-checking system as defense layers;	
Model	Limited visual understanding or feature extraction	Using auxiliary perceptual information; Using pathological/structural constraints/priors;	

tection and evaluation methods, underlying causes, and mitigation recommendations, as illustrated in Fig. 1. A summary of the main components of the report is provided in Table 1.

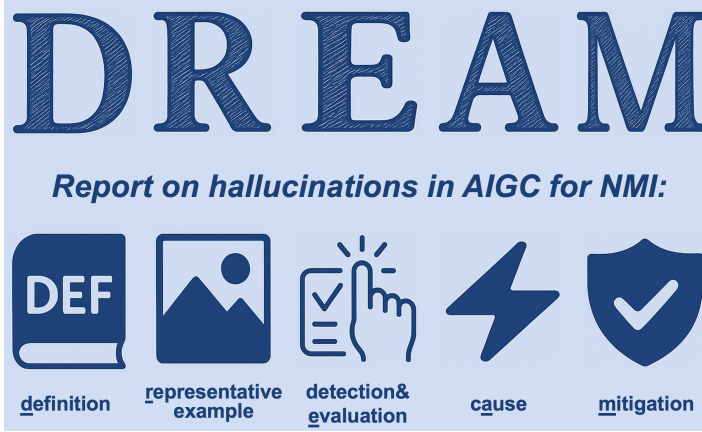


Figure 1: Organization of the DREAM report.

II Definition

The definition of hallucinations varies across publications and, in some cases, remains inconsistent or even contradictory. A precise and universally accepted definition has yet to be established (7). While hallucinations were indistinguishable from general inaccura-

cies or errors in earlier studies (8)(9), the term has gained renewed attention with the advent of large-scale models and diffusion-based architectures (4)(10)(11). The enhanced generative capabilities of these models introduce greater risks of creating misleading and fabricated content, prompting growing interest in establishing more rigorous and specific definitions of hallucinations.

In the NLP domain, hallucinations are typically defined and categorized based on their inconsistencies with real-world knowledge or the input context (12). Specifically, factual hallucinations refer to cases where AIGC contradicts verifiable real-world knowledge; faithfulness hallucinations arise when AIGC deviates from given input instructions or context. Further classifications include fact-conflicting, input-conflicting, and context-conflicting hallucinations, each describing a specific form of misalignment between the AIGC and source information (13). Additionally, (14) introduces a subset of hallucinations termed ‘confabulations’, referring to AI-generated claims that are both incorrect and arbitrary. Here, arbitrary means that model outputs fluctuate unpredictably under identical inputs due to irrelevant factors such as random seed variations. This stochastic ‘confabulation’ is distinguished from systematic hallucinations, which may arise from flawed training data.

In medical imaging, the definition of hallucinations remains ambiguous, with no consensus on its precise scope. Regarding content alteration, some studies interpret hallucinations narrowly as the addition of non-existent tissue components in AIGC (15), whereas others adopt a broader perspective that includes both the addition and removal of image structures (16)(17). This wider view en-

compasses scenarios where AI erroneously replaces real abnormalities with fabricated normal structures, such as the omission of lesions (18)(19), a case not accounted for by the narrower interpretation. From the standpoint of realism, some researchers emphasize the deceptive nature of hallucinations, defining them as realistic-looking artifacts that may mislead clinicians (20), while others expand the hallucination term to include implausible or dream-like content (21)(22). In terms of model scope, some studies propose broader definitions that also encompass artifacts introduced by traditional image reconstruction, beyond AI-specific frameworks. For example, a study on tomographic image reconstruction (23) defines hallucinations as false structures in reconstructed images that do not exist in the actual subject and cannot be stably reconstructed from acquired measurements, regardless of whether they originate from AI or conventional algorithms. In contrast, other perspectives argue that hallucinations are unique to AI and are not typically produced by traditional image processing techniques (24).

In this paper, we focus specifically on AIGC in NMI. Establishing a clear, domain-specific definition of hallucinations is critical for developing effective frameworks for detection, evaluation, and mitigation. Unlike AIGC in NLP or natural image processing, where a certain degree of creativity is acceptable, AIGC in NMI requires strict adherence to clinical anatomical and functional reality. Through an extensive literature review, we observe that most AIGC applications in NMI operate as image-to-image translation tasks. For example, tasks such as denoising or attenuation correction typically involve generating higher-quality or more quantitatively accurate images from lower-quality inputs. In such settings, implausible large-scale hallucinations, such as the addition of organs or major structures, are rarely observed. Instead, hallucinations are subtle but deceptive, typically manifesting as added small abnormalities or realistic-looking lesions that do not exist in the reference. Despite their subtlety, these added contents pose significant risks to diagnostic accuracy and therapeutic decision-making. Other types of AI-induced mistakes, such as falsely replacing abnormal regions with normal structures (e.g., omission of true lesions) or introducing consistent quantitative biases (e.g., uniform intensity shifts without visual artifacts), are considered outside the scope of hallucinations in this paper and are more appropriately categorized as general errors or biases.

Given this context, within the scope of this paper, we recommend a narrow hallucination definition in NMI: AI-generated abnormalities or artifacts that appear visually realistic and highly plausible, yet are factually false when compared to reference scans, deviating from anatomical or functional truth.

III Representative examples

In this section, we present visual examples of AIGC in NMI applications. While these generated images appear highly realistic and visually convincing, careful comparison with reference images reveals the presence of hallucinations. We illustrate cases across key tasks, including image enhancement, attenuation correction, and cross-modality image translation, demonstrating how subtle yet deceptive artifacts can emerge in these AI-driven processes. These hallucinations are often difficult to detect, potentially misleading

clinical interpretation.

III.1 Image enhancement

The advent of AI has introduced a variety of image enhancement techniques for denoising, deblurring, and partial-volume correction in PET and SPECT imaging, enabling purely software-based improvements in image quality (1). Numerous studies (25)(26) have investigated AI-driven translation from low-count/high-noise to high-count/low-noise images, offering the potential to reduce radiation exposure, shorten scan durations, and lower scanner costs. AI-based enhancement methods have shown impressive performance, often producing images that are visually compelling and nearly indistinguishable from high-quality reference scans.

However, hallucinations can occasionally emerge, distorting underlying anatomical or functional information. Fig. 2 presents examples of hallucinations in AI-driven PET and SPECT denoising, highlighting instances where AI-generated outputs unintentionally alter critical imaging details.

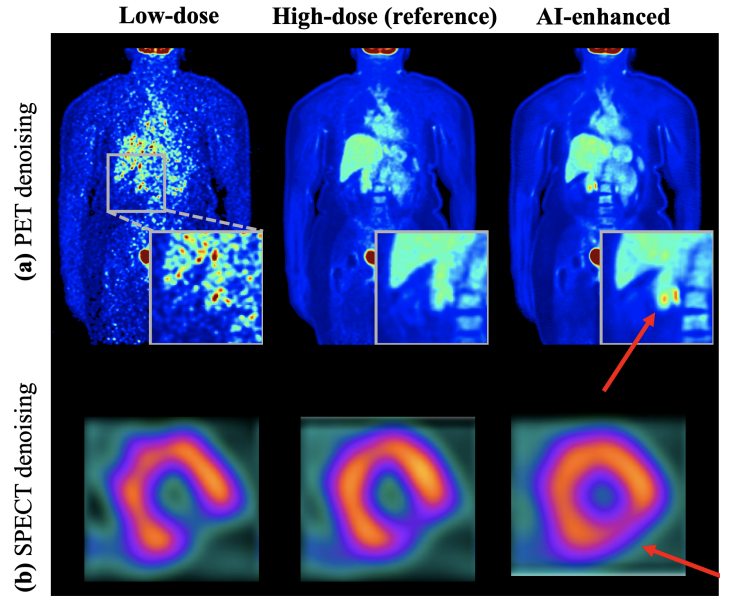


Figure 2: Examples of hallucinations in AI-driven image enhancement. **(a)** PET image denoising generated false lesions using the method proposed in (27). **(b)** SPECT image denoising generated false negative perfusion images (reprinted from (26), licensed under CC BY 4.0). Red arrows indicate AI-introduced hallucinations.

III.2 Attenuation correction

Attenuation correction (AC) is essential for producing quantitatively accurate PET and SPECT images, traditionally relying on CT-based attenuation maps. However, certain dedicated imaging systems, such as PET/MRI scanners and SPECT-only scanners, lack integrated CT, making conventional AC methods impractical. Further, CT-based attenuation maps involve additional radiation dose to the patient, which in some cases may be poorly justified or even contraindicated. To address these limitations, researchers have developed AI-based AC techniques, which estimate AC im-

ages directly from non-AC images, eliminating the need for additional reconstruction steps.

Fig. 3 presents examples of AI-driven AC in both PET and SPECT imaging. While the AI-generated images appear visually accurate, a closer comparison with reference images (CT-AC images) reveals the presence of hallucinations, manifesting as false activity patterns that do not correspond to actual anatomical or functional structures. These hallucinated artifacts introduce misleading visual cues that may negatively impact diagnostic accuracy.

Figure 3: Examples of hallucinations in NMI with AI-driven CT-free attenuation correction (AC): (a) for PET imaging, showing generated false abnormality in the brain region (please refer to Fig. 2b in (28)); and (b) for SPECT imaging, showing generated false negative perfusion (please refer to Fig. 7a in (29)).

III.3 Cross-modality translation

AI-driven cross-modality image translation is being explored to generate images of one modality from another, addressing scenarios where two complementary imaging modalities are required, but only one scanner is available. For example, it has been argued that generating PET images from CT or MRI (30)(31) offers potential opportunities to mitigate PET’s high costs and radiation exposure, thereby reducing medical examination expenses and associated health risks for patients, although such claims have yet to be robustly proven clinically. Perhaps more importantly, cross-modality image translation may be able to support multicenter studies (3) by harmonizing data from institutions that have limited access to different imaging modalities, and can help address data scarcity by generating synthetic image datasets.

Fig. 4 presents examples of AI-driven cross-modality image translation, including MRI-PET, PET-CT, and PET-SPECT conversions. While these advancements highlight the promising capabilities of AI in cross-modality imaging, they also underscore the risk of hallucinations, which can introduce clinically significant or scientifically important errors.

IV Detection and evaluation methods

Detecting and evaluating hallucinations is vital for reliable validation and clinical deployment of AIGC in NMI. Further, establishing quantitative measures of hallucination can help define a minimum acceptable degree for AI processing, like the lowest dose thresholds for AI-based denoising. Such thresholds would balance the extent of dose reduction with the risk of AI-induced hallucinations, ensuring that the benefits of AI-enhanced image quality do not come at the cost of inaccurate representations.

To systematically assess hallucinations, we recommend adopting

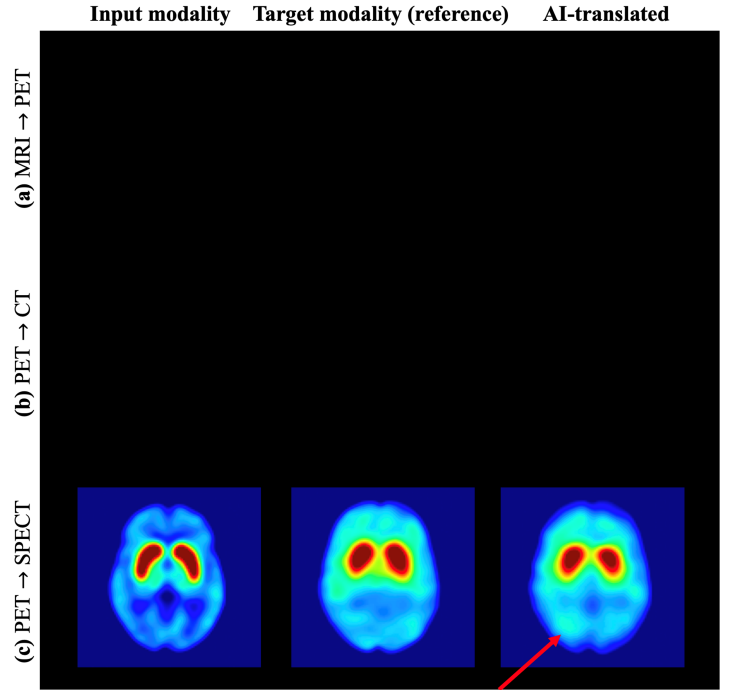


Figure 4: Examples of hallucinations in AI-driven cross-modality image translation. (a) MRI-PET translation (please refer to Fig. 1 in (30)). While visually realistic, the AI-generated PET image exhibits falsely increased glucose uptake in the temporoparietal lobe, which could potentially lead to misdiagnosis of Alzheimer’s disease. (b) PET-CT translation (please refer to Fig. 7 in (3)). (c) PET-SPECT translation (reprinted from (32), licensed under CC BY 4.0). Red arrows highlight AI-induced hallucinations.

multifaceted metrics, which may draw upon methodologies from recent studies in other domains and be adapted to the specific context of NMI. Below, we outline several examples and preliminary ideas; however, further research is essential to develop accurate and widely accepted evaluation frameworks tailored to this field.

IV.1 Image-based metric

When paired reference images are available for evaluating AIGC performance, the hallucination index has been proposed to detect synthesized spurious features (24). This index is computed as the Hellinger distance between the distribution of AIGC and a so-called ‘zero-hallucination reference’. This reference approximates a hallucination-free image, by adding adaptive white Gaussian noise to the reference image, with noise power calibrated to match the signal-to-noise ratio (SNR) of the AIGC. Since the Hellinger distance is sensitive to discrepancies in distribution tails, this method is suited for detecting false-positive lesions, i.e., rare and high-intensity voxels that might distort the distribution tails. However, the original formulation of the hallucination index was specifically tailored for Fourier diffusion-based models, where the noise power is inferred from a diffusion bridge between output and reference images. This limits the metric’s applicability to broader AI generative situations.

To broaden the applicability of the hallucination index across

diverse AI model architectures in NMI, we think several computational refinements can be considered. Taking whole-body PET denoising as an example, the SNR estimation method proposed in (33)(34) can be adopted to align the SNR of high-count reference image with that of the AIGC, facilitating the construction of a comparable ‘zero-hallucination reference’. Specifically, the SNR is calculated as the ratio of the mean to the standard deviation of voxel intensities within a uniform spherical region of interest (ROI), typically 3 cm in diameter and placed in biologically stable organs such as the liver. Adaptive white Gaussian noise is then added to the image with lower SNR, either the high-count reference or the AIGC, so that the SNRs between the two are aligned. Given the large size of whole-body PET images, a single SNR measurement is inadequate to capture spatial variability. Therefore, hallucination index should be computed over smaller patches or other appropriately sized subregions. A visual demonstration is presented in Fig. 5, where the hallucination index is computed for denoised outputs from two different models. The results show that a lower hallucination index is associated with fewer hallucinated artifacts, supporting the metric’s potential utility as a quantitative tool for assessing AI-induced hallucinations in NMI.

Even so, several limitations of the above hallucination index formulation must be acknowledged. First, while the index can be used for relative comparisons between different generated results, where a lower value may suggest fewer hallucinations, the interpretation of its absolute value remains ambiguous. Specifically, it is unclear what value range constitutes severe hallucinations or what threshold might be deemed clinically unacceptable. Second, the construction of a ‘zero-hallucination reference’ by adding white Gaussian noise cannot accurately account for complex characteristics in PET imaging, which may be better modeled by Poisson or mixed Poisson-Gaussian distributions. Moreover, the current SNR estimation reflects only local noise behavior and may fail to reflect variability outside the selected ROI. Third, the current formulation does not consider anatomical context or clinical relevance of hallucinations. For instance, hallucinated lesions or hot spots in critical organs such as the liver or lungs could have a much greater diagnostic impact in FDG oncology imaging than similar artifacts in less critical regions like the bowel. A potential improvement could be incorporating organ segmentation maps into the index calculation, enabling spatially weighted assessments that emphasize hallucinations in diagnostically important areas. In summary, substantial research is still needed to develop a more representative and broadly applicable hallucination index in NMI.

Radiomics analysis has also been explored as an evaluation method for AIGC (35). In this approach, diagnostically relevant ROIs are selected from critical anatomical areas, and radiomic features are extracted from both the AI-generated and reference images. Statistical comparisons between these feature sets can reveal whether the AIGC is consistent with the reference; significant discrepancies may indicate the presence of hallucinations.

However, not all radiomics-based discrepancies necessarily correspond to hallucinations. Other types of errors that fall outside the scope of hallucinations defined in this paper, such as lesion omission or general biases like uniform intensity shifts (as discussed in Section II), can also contribute to radiomics differences. There-

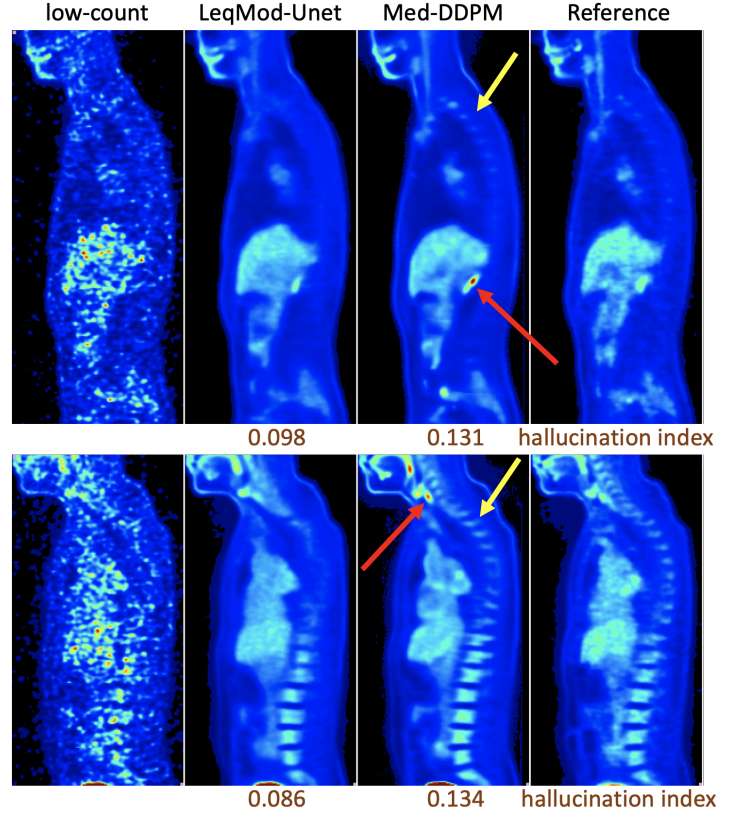


Figure 5: Examples of hallucination index computation in PET image denoising. From left to right: input low-count images, denoised results using LeqMod-Unet (25) and Med-DDPM (27), and the high-count reference image. The hallucination index between each AI-generated image and the reference is displayed below the image, enabling a quantitative comparison. Notably, the diffusion-based Med-DDPM produces results with clearer anatomical structures and higher visual quality (highlighted by yellow arrows), but it also demonstrates a greater tendency to hallucinate false content (indicated by red arrows).

fore, further research is needed to identify radiomic features that are specifically sensitive to hallucinations, while minimizing confounding effects from other non-hallucinatory errors.

IV.2 Dataset-based metric

For cases where paired reference images are unavailable, the neural hallucination precursor was developed (21). This method quantifies hallucinations from a feature-space perspective, based on the assumption that false content arises from misrepresented features. The metric measures the k-nearest neighbor distance between the intermediate feature embeddings of the AIGC and a ‘hallucination-free feature bank’. The feature bank is pre-constructed using a calibration dataset sampled from the training set, ensuring that it captures a true distribution of target features.

Nevertheless, the neural hallucination precursor is model-dependent, as the ‘hallucination-free feature bank’ is defined and obtained by a specific model architecture. This dependence limits its applicability for comparing hallucination levels across different

AI models, as each model may employ distinct feature extraction mechanisms that shape the learned feature distributions differently.

To rank different methods in the absence of reference images, the concept of no-gold-standard evaluation (NGSE) (36) may offer insights. Although NGSE was originally developed to assess conventional quantitative imaging techniques, its framework could potentially be adapted for AIGC evaluation. This approach models a linear stochastic relationship between the measured values and unknown true values, which are assumed to follow a four-parameter beta distribution. It then estimates the model parameters by maximizing the likelihood of the observed data and derives the noise-to-slope ratio from these estimates to quantify the precision of each method (36). When applying this framework to AIGC evaluation, quantitative values could be metrics such as the mean or maximum activity concentration within specific ROIs in the AI-generated images.

However, two key challenges arise. First of all, the assumption of linearity between true and measured values may not hold when nonlinear generative models are involved in the process. Second, and as previously noted, this metric may capture general errors, rather than hallucinations specifically. Adapting it to isolate hallucinations from other non-hallucinatory deviations will require substantial methodological refinement.

IV.3 Clinical task-specific metric

Ensuring the clinical applicability of AIGC is essential for its successful integration into medical practice. Therefore, clinically relevant tools for hallucination detection and evaluation are necessary to meet the requirements of real-world deployment.

One strategy evaluates hallucinations through downstream segmentation or classification tasks (37). Task-specific observers, either expert radiologists or pre-trained disease classifiers/segmenters, analyze both the AIGC and reference images. Their decisions across the two images are then compared to identify potential hallucinations. For example, in a denoising evaluation study (35), expert readers performed lesion segmentation on both denoised and high-dose images. The Dice coefficient was calculated to quantify segmentation agreement, serving as a key hallucination indicator. If a hallucinated lesion appears in the denoised image, the resulting segmentation mismatch would yield a reduced Dice score. Inevitably, this strategy has limitations. Human reading is time-consuming and often infeasible for large-scale datasets, while automated observers may introduce their own errors, potentially confounding accurate hallucination detection.

Another strategy is to have medical professionals directly assess the AIGC using clinically relevant criteria, such as disease-specific image features (5)(38). In several studies (35)(39), physicians rated AIGC using a 5-point Likert scale: 5 (Excellent): no detectable hallucinations; high diagnostic quality. 4 (Good): minor hallucinations; acceptable for clinical interpretation. 3 (Average): noticeable hallucinations but still interpretable (e.g., added lesions/artifacts in diagnostically irrelevant regions). 2 (Below Average): significant hallucinations that impair interpretation. 1 (Poor): severe hallucinations; unsuitable for clinical use. Naturally, a 5-point scale alone is insufficient to fully capture the complexity of hallucinations in AIGC for NMI. A more informative approach could incorporate

bounding box annotations to localize hallucinations, accompanied by brief descriptive text (e.g., ‘a false, small lesion-like hot spot is present at the apex of the liver’) alongside the Likert scale rating. Such annotations are more feasible for physicians than full voxel-wise segmentation, and still provide valuable granularity for hallucination assessment. Still, the accuracy of these evaluations often depends on access to reference images. Without them, even expert readers may be misled by highly realistic hallucinations. Additionally, since it is impractical to have physicians review unlimited AIGC cases, determining an adequate and representative sample size for evaluating hallucination performance remains a key challenge.

IV.4 Automatic hallucination detector

To reduce human labor in hallucination assessment, automatic hallucination detectors have recently been explored in large (vision) language models (L(V)LMs), supported by the development of hallucination benchmark datasets (40). For example, the MedHallMark dataset (4) comprises paired input images and LVLM-generated text, each annotated by human experts for hallucinations. Annotations categorize outputs into six levels: catastrophic, critical, attribute, prompt-induced, minor, and correct statements, each assigned a weight by a proposed MediHall score: 0.0, 0.2, 0.4, 0.6, 0.8, and 1.0, respectively. A higher MediHall score indicates fewer hallucinations. Using this annotated dataset, a MediHall detector was trained to automatically classify hallucination severity and output corresponding MediHall scores for LVLM-generated medical text. In the vision domain, frameworks such as AQuA (16) have been developed to assess hallucinations in AI-driven image translation tasks. AQuA introduces various morphological hallucinations and error types into translated images, which were then manually annotated and labeled as acceptable or unacceptable. A dedicated model, AQuA-Net, was subsequently trained on this dataset to automate hallucination detection and assess the reliability of generated results.

There is currently no hallucination-annotated benchmark dataset curated for NMI applications, to the best of our knowledge. This highlights an urgent need for the research community to collaboratively develop such a resource, ideally through multi-institutional efforts. One promising approach involves leveraging crowdsourcing platforms to collect a diverse set of AI-generated NMI images that exhibit hallucinations, along with expert annotations. These annotations could be guided by standardized criteria, such as bounding boxes to indicate hallucination locations, brief descriptive text, and Likert-scale ratings for severity, as discussed in Section IV.3. Of course, the final annotation protocol will require further discussion and consensus to ensure consistency and clinical relevance. The dataset could be designed for continuous expansion, accommodating new contributions over time. Establishing such a standardized hallucination benchmark dataset for NMI would lay a critical foundation for systematic detection, evaluation, and mitigation.

V Causes and mitigation recommendations

Most AIGC applications in NMI can be formulated as image-to-image estimation tasks, where the objective is to learn a mapping function from a source domain S to a target domain T , denoted as $G : S \rightarrow T$. Given a training dataset \mathcal{D} with marginal distributions P_S and P_T , the goal is to identify an optimal approximation: $\hat{G} = \arg \min_{\hat{G} \in H} \mathcal{L}(\hat{G}, \mathcal{D})$, where \mathcal{L} is the loss function and H the hypothesis space (21). Hallucinations arise when the learned mapping function \hat{G} deviates from the true underlying mapping G . The mechanisms and causes of hallucinations are complex and multifaceted, and mitigation strategies must be tailored to their specific causes, encompassing data quality, training paradigms, and model architecture (15)(37).

V.1 Data perspective

V.1.1 Domain shift

Domain shift, a mismatch between data distribution used for AI model training and that encountered at testing (i.e., test sample $s \notin P_S$), is widely recognized as a key contributor to hallucinations (5)(6)(17). Since generative AI models rely heavily on learned statistical priors, any deviation between training and testing distributions can result in unpredictable outputs, increasing the risk of hallucinations. For instance, over-representation of certain patterns in training data (e.g., lesions frequently occurring in the liver) may lead the model to erroneously hallucinate such features in test samples where they do not exist (10)(41). Conversely, under-representation of certain pathological scenarios may impair the model’s performance on out-of-distribution samples, resulting in synthesized artifacts that do not correspond to actual medical conditions. A model trained primarily on healthy subjects, for instance, may hallucinate features when applied to rare diseases by extrapolating from incomplete or biased representations (19)(22).

To mitigate hallucinations caused by domain shift, several strategies can be considered. **First**, usage guidelines should clearly define the intended scope and limitations of AI models, to prevent hallucinations caused by inappropriate or unintended applications. **Second**, improving the quality, quantity, and diversity of training data, by including a wider range of scanners, imaging protocols, and patient populations, can reduce hallucination risk. Fig. 6 (a) illustrates how richer and more comprehensive training datasets effectively decrease hallucinated artifacts. In this study (42), a federated network trained on datasets from three institutions outperformed that trained on a single institution dataset. **Third**, when large-scale datasets are unavailable for training, domain adaptation techniques become useful. For instance, in (43), to handle PET denoising across arbitrary noise levels with training data limited to a narrow noise range, an adversarial domain generalization method was employed. This method used a continuous discriminator to classify noise levels, thereby minimizing distribution shifts in latent feature representations across different noise domains. As shown in Fig. 6 (b), the model incorporating this technique demonstrated reduced hallucinations compared to that trained without it. **Fourth**, transfer learning offers another effective solution by leveraging publicly pre-trained models followed by fine-tuning on local data, striking a balance between generaliza-

tion and specialization. For example, in (44), a pre-trained FDG PET denoising model was fine-tuned on only three Zr-89 CD8 ImmunoPET scans, enabling effective adaptation to a tracer-scarce target task. Under similar ideas, the concept of continuous dataset updating has been proposed, where models are regularly fine-tuned with newly acquired data to keep up with evolving clinical scenarios (13). However, such methods come with additional training costs and the potential risk of catastrophic forgetting. **Fifth**, retrieval-augmented generation (RAG) provides an inference-time solution that improves output quality without retraining. For example, (45) reformulated complex medical questions into search-optimized synthetic queries, retrieving external knowledge from online databases to improve output quality. However, unlike language tasks, RAG for NMI is currently limited due to the lack of well-structured, publicly available visual knowledge sources.

As discussed, each potential mitigation strategy presents advantages and limitations, particularly when applied to NMI. Substantial adaptation and continued research are needed to tailor these approaches to the unique challenges of this field.

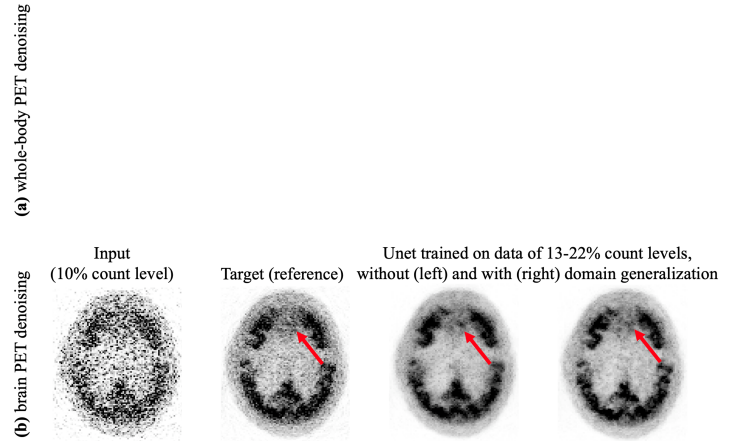


Figure 6: Examples of hallucination mitigation through the use of (a) richer and higher-quality training data for ^{18}F -FDG whole-body PET denoising (please refer to Fig. 3 in (42)), and (b) a domain generalization technique for ^{18}F -MK-6240 brain PET denoising (adapted from (43) @Institute of Physics and Engineering in Medicine. Reproduced by permission of IOP Publishing. All rights reserved.).

V.1.2 Data nondeterminism

The mapping function $G : S \rightarrow T$ is inherently nondeterministic due to aleatoric uncertainty in the dataset \mathcal{D} (21). This nondeterminism arises from random variability in data acquisition processes, including measurement noise and stochastic fluctuations during image formation. The intrinsic ill-posedness of the estimation problem $\hat{G} = \arg \min_{\hat{G} \in H} \mathcal{L}(\hat{G}, \mathcal{D})$, given the dataset \mathcal{D} , results in one-to-many mappings for $G(s)$, where multiple plausible solutions may exist and many of them do not reflect the true observations. Consequently, this ambiguity can give rise to hallucinations.

To mitigate hallucinations caused by nondeterministic mappings, several strategies may be considered. **First**, optimizing data acquisition can help produce high-quality and consistent datasets, thereby establishing a more reliable foundation for model training. However, implementing this in practice is challenging, as it requires access to high-performance scanners and the ability to execute ultra-high-quality imaging protocols, particularly difficult for modalities such as SPECT and planar imaging. **Second**, applying rigorous data preprocessing, such as systematic data cleaning, can reduce inconsistencies and improve overall data fidelity. Nonetheless, this demands a lot of work, and establishing clear and objective criteria for determining whether the data meet quality standards remains a complex issue.

In summary, although addressing aleatoric uncertainty at the data level holds promise for reducing hallucination risks, its practical implementation is often constrained by the high costs of hardware and operational complexity of data acquisition.

V.1.3 Input perturbations or imperfect prompts

Even in well-trained and high-performing AI models, hallucinations may still arise due to input perturbations or suboptimal prompts (46). Prompt engineering seeks to improve output accuracy by optimizing the structure and content of input instructions (20). Carefully formulated prompts that clearly define response boundaries and expectations help reduce ambiguity and guide the model toward more precise and reliable outputs (13). For instance, (47) introduced structured text prompts that explicitly specify organs and anatomical structures in the image, thereby enhancing the anatomical fidelity of denoised PET results. The accuracy of prompts plays a critical role in the model success. Similarly, (48) employed dual prompts, one indicating noise count level and another providing a general denoising directive, to improve PET denoising across varying count levels.

V.2 Learning perspective

The inherent probabilistic nature of AI models makes hallucinations inevitable to some extent, analogous to the concept of epistemic uncertainty. AI models \hat{G} rely on pattern recognition and statistical inference from training data, without a true understanding of meaning or facts. Consequently, hallucinations emerge as a fundamental limitation of data-driven learning systems (21). This inevitability arises from underspecification, where many candidate solutions \hat{G} within the Rashomon set H^* can equally satisfy the training objective, i.e., $\mathcal{L}_{val}(\hat{G}, \mathcal{D}) < \tau, \forall \hat{G} \in H^*$, where \mathcal{L}_{val} is the validation criteria and τ a predefined threshold. The Rashomon set $H^* \subset H$ comprises all models that achieve near-optimal performance within the possible space H (21). Despite fitting the data well, these solutions may not align with the true underlying function, expressed as $\hat{G} \neq G$. Without a theoretical basis to prefer one solution over another, the randomly selected function \hat{G} may deviate from ground truth, particularly in cases of small datasets or under-constrained generative frameworks such as unsupervised learning.

To mitigate this kind of hallucination, several techniques can be considered. **First**, ensemble model averaging or feature averaging, which aggregates outputs or latent features from multiple runs of

models with similar architectures (i.e., multiple qualified \hat{G} candidates), can reduce uncertainty and produce more stable results with fewer hallucinated artifacts. For example, in translating non-AC low-dose PET images into AC standard-dose PET images, (49) averaged outputs from three 2.5D diffusion models across axial, sagittal, and coronal views, achieving better results compared to a single model run. Likewise, injecting random noise into inputs and averaging the resulting vision features across multiple runs has been shown to suppress spurious signals and improve reliability in medical image translation tasks (50). However, these averaging strategies incur high computational cost due to the need for multiple model runs. **Second**, user-guided interactive alignment may be especially valuable in the safety-critical context of NMI. This human-in-the-loop strategy uses iterative expert feedback to guide model learning toward better understanding of real-world facts (51). Practically, it involves incorporating human knowledge to interactively select the most plausible \hat{G} solution from a pool of candidates. While effective, this method is labor-intensive and subject to inter-observer variability. **Third**, to alleviate human workload, automated fast-checking systems have been developed to simulate expert feedback and interactions (13)(52). These systems leverage predefined rules, statistical heuristics, or learned hallucination detectors (as discussed in Section IV.4), to flag potentially erroneous content in model outputs. Serving as an auxiliary verification layer or adversarial critic, these systems enhance the reliability and interpretability of AI-generated outputs. Nevertheless, the effectiveness of this approach depends on the accuracy and robustness of the checking system itself.

V.3 Model perspective

The interpretation of complex visual scenes by AI involves multiple layers of abstraction, which complicates the diagnosis and correction of errors. A key contributor to hallucinations is the model’s limited capacity for visual understanding and feature learning, both of which directly impact the reliability of its outputs.

Improving the perceptual capability of vision encoders can be achieved through more context-appropriate architectural designs and the integration of additional perceptual information, such as semantic maps or multi-modality representations. For example, a pathology-aware translation model was proposed for MRI-PET image translation (30). It used adaptive group normalization layers to integrate multi-modal conditions, including demographic information, cognitive scores, and Alzheimer’s disease biomarkers. These fused multi-modal priors enhanced the preservation of pathological features in the generated PET images, compared to the baseline model without such conditioning, as illustrated in Fig. 7 (a). In addition, incorporating strong anatomical and functional constraints, either through auxiliary encoders or specialized loss functions, has shown promise in reducing hallucinations by guiding more robust feature extraction (50). For example, in (53), an anatomically and metabolically informed diffusion model was introduced for PET denoising. This model incorporated lesion and organ segmentation maps as auxiliary constraints to regularize the denoising process, improving structural fidelity in generated PET images (Fig. 7(b)). Similarly, in (54), a task-specific loss term was added to a baseline SPECT denoising model, incorporating performance on perfusion

defect detection as an auxiliary supervision signal. This addition helped suppress hallucinations in the denoised outputs, as shown in Fig. 7(c). While effective, these approaches often incur additional computational cost due to the integration of complex priors and regularization mechanisms.

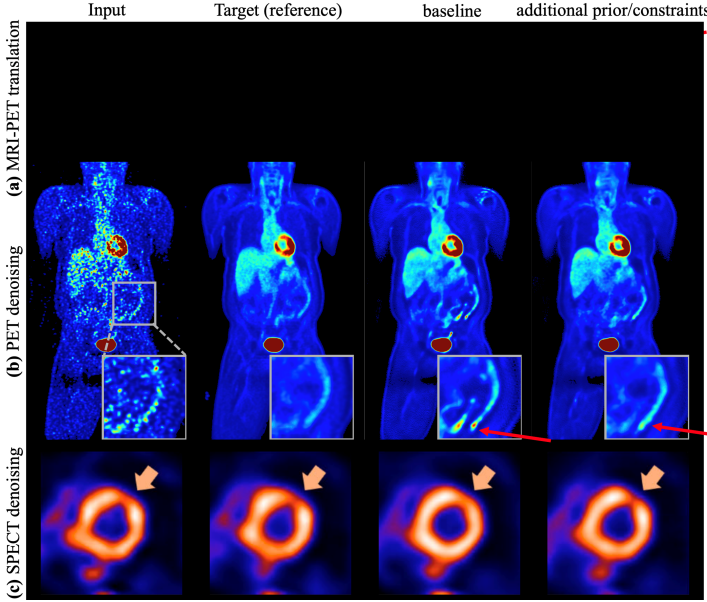


Figure 7: Examples of hallucination mitigation using additional constraints or priors. (a) MRI-to-PET translation incorporating multi-modal and clinical prior information (please refer to Fig. 1 in (30)). (b) PET denoising using anatomical and metabolic priors to regularize generation (53). (c) SPECT denoising guided by a task-specific loss function informed by perfusion defect detection (reprinted from (54), licensed under CC BY 4.0).

VI Future work

Despite the recommendations and insights outlined above, substantial work remains to be done. The strategies presented may encounter limitations when applied to specific NMI scenarios. Continued research and targeted adaptation are crucial to address the unique characteristics and complexities of hallucinations in NMI.

A foundational next step toward standardizing hallucination detection may be the development of a publicly available, large-scale benchmark dataset tailored for AIGC in NMI. This dataset should include AI-generated NMI images, ideally paired with reference images when available, but also accommodating unpaired cases, and most importantly, be accompanied by structured hallucination annotations. The diversity of existing generative models across various NMI applications provides a solid foundation for curating such a resource, which in turn could support the development and validation of automated hallucination detectors. Several critical considerations must be addressed in constructing such a benchmark. **First**, while an ideal benchmark would span multiple NMI modalities, significant differences in tracer characteristics, imaging resolutions, and diagnostic contexts make cross-modality stan-

dardization challenging. A more practical approach may involve developing modality-specific benchmarks as an initial step, followed by gradual integration. **Second**, establishing a consensus annotation protocol is essential. As discussed in Sections IV.3 and IV.4, annotations could include bounding boxes for localization, short descriptive texts summarizing hallucination characteristics, and Likert-scale scores to reflect severity and diagnostic impact. When feasible, richer annotations such as lesion segmentations or disease classifications, especially for those likely to be influenced by hallucinations, could be incorporated. To reduce annotation burden, an interactive annotation loop can be employed, combining expert-reviewed samples, trained hallucination detectors, and visualization tools to enable scalable annotation with human oversight. **Third**, the benchmark should support computational evaluation metrics in addition to human annotations. Existing methods such as the hallucination index and NGSE (Sections IV.1 and IV.2) provide initial references, but they do not adequately isolate hallucinations from general errors. New metrics should be developed based on features or statistical patterns that are specifically sensitive to hallucinations, while remaining robust against non-hallucinatory errors. Importantly, such metrics should reflect anatomical and clinical relevance, potentially by assigning greater weights to hallucinations in diagnostically critical regions (e.g., liver, lungs) compared to those in less critical areas (e.g., bowel). **Fourth**, hallucination evaluation in cases without reference images remains particularly challenging. In these scenarios, both expert readers and automatic detectors may be misled by highly realistic outputs. Here, inter- and intra-observer variability could serve as an auxiliary signal, capturing uncertainty or disagreement among clinicians in interpreting potential hallucinations. **Fifth**, the design of hallucination detector architectures warrants further investigation. Ideally, models should handle AIGC inputs with and without references, and support multi-headed outputs to jointly predict hallucination presence, spatial location, descriptive attributes, severity scores, and possibly task-specific misinterpretation risks. Fine-tuning existing LVLs may be a promising direction; however, most LVLs are optimized for natural 2D images, so adapting them to volumetric NMI remains a key technical hurdle.

On the mitigation side, while access to high-quality and large-scale training data remains ideal for hallucination mitigation, it is often impractical in NMI due to limited data availability and the inherent variability in real-world acquisitions (as noted in Section V.1.2). Therefore, future research should prioritize data-efficient and generalizable strategies. Several directions merit further exploration. For instance, transfer learning from high-resource modalities or the application of domain adaptation techniques could enhance generalizability when training data are limited. Moreover, although RAG techniques are primarily applied in NLP, they hold potential for vision tasks. The curated hallucination benchmark dataset could serve as a retrieval repository to guide generation toward more grounded outputs. Additionally, integrating automated hallucination detectors into the model training process represents another promising direction. For example, hallucination-aware loss functions, such as adversarial terms informed by hallucination detector feedback, could be employed to penalize hallucination-prone generations during training. These approaches may help proac-

tively suppress hallucinations and enhance the reliability of AIGC systems in NMI.

Lastly, integrating hallucination detection and correction into clinical pipelines remains a critical and unexplored frontier, requiring the deployment of hallucination screening tools and hallucination-aware AI systems for real-world clinical use.

VII Conclusion

Hallucinations in artificial intelligence-generated content (AIGC) for nuclear medicine imaging (NMI) remain a critical challenge, with significant implications for clinical diagnostic accuracy and patient management. In this paper, we introduce the DREAM report, which offers a comprehensive perspective on hallucinations in AIGC for NMI. These hallucinations may arise from biased or non-deterministic data, the intrinsic probabilistic nature of deep learning, or limited visual feature understanding by models. Effective detection and evaluation require multi-faceted frameworks, incorporating image-based, dataset-based, and clinical task-based metrics, as well as the development of automated detectors trained on hallucination-annotated datasets. Mitigation strategies must be tailored to the specific causes of hallucinations and should involve enhancements in data quality, learning methodologies, and model architectures to improve the robustness, reliability, and clinical applicability of AI-driven systems in NMI. This DREAM report serves as a starting point for discussions in the field, highlighting the need for continued and extensive research.

Disclosure

This work was supported by the National Institutes of Health (NIH) under grants R01CA275188 and P41EB022544. No other potential conflict of interest relevant to this article was reported.

References

- Balaji V, Song TA, Malekzadeh M, Heidari P, Dutta J. Artificial intelligence for PET and SPECT image enhancement. *J Nucl Med*. 2024;65:4–12.
- Lee JS. A review of deep-learning-based approaches for attenuation correction in positron emission tomography. *IEEE Trans Radiat Plasma Med Sci*. 2020;5:160–84.
- Armanious K, Jiang C, Fischer M, et al. MedGAN: medical image translation using GANs. *Comput Med Imaging Graph*. 2020;79:101684.
- Chen J, Yang D, Wu T, et al. Detecting and evaluating medical hallucinations in large vision language models. *arXiv preprint*. arXiv:2406.10185; 2024.
- Rawte V, Sheth A, Das A. A survey of hallucination in large foundation models. *arXiv preprint*. arXiv:2309.05922; 2023.
- Liu H, Xue W, Chen Y, et al. A survey on hallucination in large vision-language models. *arXiv preprint*. arXiv:2402.00253; 2024.
- Sun Y, Sheng D, Zhou Z, Wu Y. AI hallucination: towards a comprehensive classification of distorted information in artificial intelligence-generated content. *Humanit Soc Sci Commun*. 2024;11:1–14.
- Zhang W, Wang YX. Hallucination improves few-shot object detection. In: *Proceedings of the IEEE/CVF Conference on Computer Vision and Pattern Recognition*. 2021:13008–17.
- Li K, Zhang Y, Li K, Fu Y. Adversarial feature hallucination networks for few-shot learning. In: *Proceedings of the IEEE/CVF Conference on Computer Vision and Pattern Recognition*. 2020:13470–9.
- Li Y, Du Y, Zhou K, Wang J, Zhao WX, Wen JR. Evaluating object hallucination in large vision-language models. *arXiv preprint*. arXiv:2305.10355; 2023.
- Aithal SK, Maini P, Lipton Z, Kolter JZ. Understanding hallucinations in diffusion models through mode interpolation. In: *Advances in Neural Information Processing Systems*. Vol. 37. 2024:134614–44.
- Vishwanath PR, Tiwari S, Naik TG, et al. Faithfulness hallucination detection in healthcare AI. In: *KDD 2024 Workshop AIDSH*. 2024.
- Gadiko A. Understanding and addressing AI hallucinations in healthcare and life sciences. *Int J Health Sci*. 2024;7:1–11.
- Farquhar S, Kossen J, Kuhn L, Gal Y. Detecting hallucinations in large language models using semantic entropy. *Nature*. 2024;630:625–30.
- Gottschling NM, Antun V, Hansen AC, Adcock B. The troublesome kernel: on hallucinations, no free lunches, and the accuracy-stability tradeoff in inverse problems. *SIAM Review*. 2025;67:73–104.
- Huang L, Li Y, Pillar N, Haran TK, Wallace WD, Ozcan A. Autonomous quality and hallucination assessment for virtual tissue staining and digital pathology. *arXiv preprint*. arXiv:2404.18458; 2024.
- Cohen JP, Luck M, Honari S. Distribution matching losses can hallucinate features in medical image translation. In: *Med Image Comput Comput Assist Interv*. Springer. 2018:529–36.
- Muckley MJ, Riemenschneider B, Radmanesh A, et al. Results of the 2020 fastMRI challenge for machine learning MR image reconstruction. *IEEE Trans Med Imaging*. 2021;40:2306–17.
- Kim S, Jin C, Diethe T, et al. Tackling structural hallucination in image translation with local diffusion. In: *Proceedings of the European Conference on Computer Vision*. Springer. 2024:87–103.
- Zhang P, Shi J, Kamel Boulos MN. Generative AI in medicine and healthcare: moving beyond the ‘peak of inflated expectations’. *Future Internet*. 2024;16:462.
- Oh JH, Falahkheirkhah K, Bhargava R. Detecting hallucinations in virtual histology with neural precursors. *arXiv preprint*. arXiv:2411.15060; 2024.

22. Hatem R, Simmons B, Thornton JE. A call to address AI “hallucinations” and how healthcare professionals can mitigate their risks. *Cureus*. 2023;15.
23. Bhadra S, Kelkar VA, Brooks FJ, Anastasio MA. On hallucinations in tomographic image reconstruction. *IEEE Trans Med Imaging*. 2021;40:3249–60.
24. Tivnan M, Yoon S, Chen Z, Li X, Wu D, Li Q. Hallucination index: an image quality metric for generative reconstruction models. In: *Med Image Comput Comput Assist Interv*. Springer. 2024:449–58.
25. Xia M, Xie H, Liu Q, et al. LpQcM: adaptable lesion-quantification-consistent modulation for deep learning low-count PET image denoising. *arXiv preprint*. arXiv:2404.17994; 2024.
26. Aghakhan Olia N, Kamali-Asl A, Hariri Tabrizi S, et al. Deep learning-based denoising of low-dose SPECT myocardial perfusion images: quantitative assessment and clinical performance. *Eur J Nucl Med Mol Imaging*. 2022:1–15.
27. Dorjsembe Z, Pao HK, Odonchimed S, Xiao F. Conditional diffusion models for semantic 3D brain MRI synthesis. *IEEE J Biomed Health Inform*. 2024;28:4084–93.
28. Shiri I, Ghafarian P, Geramifar P, et al. Direct attenuation correction of brain PET images using only emission data via a deep convolutional encoder-decoder (Deep-DAC). *Eur Radiol*. 2019;29:6867–79.
29. Yang J, Shi L, Wang R, et al. Direct attenuation correction using deep learning for cardiac SPECT: a feasibility study. *J Nucl Med*. 2021;62:1645–52.
30. Li Y, Yakushev I, Hedderich DM, Wachinger C. PASTA: pathology-aware MRI to PET cross-modal translation with diffusion models. In: *Med Image Comput Comput Assist Interv*. Springer. 2024:529–40.
31. Zheng X, Worhunsky P, Liu Q, et al. Generating synthetic brain PET images of synaptic density based on MR T1 images using deep learning. *EJNMMI physics*. 2025;12:30.
32. Lopes L, Jiao F, Xue S, et al. Dopaminergic PET to SPECT domain adaptation: a cycle GAN translation approach. *Eur J Nucl Med Mol Imaging*. 2025;52:851–63.
33. Chang T, Chang G, Clark Jr JW, Diab RH, Rohren E, Mawlawi OR. Reliability of predicting image signal-to-noise ratio using noise equivalent count rate in PET imaging. *Med Phys*. 2012;39:5891–900.
34. Yan J, Schaefferkoetter J, Conti M, Townsend D. A method to assess image quality for low-dose PET: analysis of SNR, CNR, bias and image noise. *Cancer Imaging*. 2016;16:1–12.
35. Patwari M, Gutjahr R, Marcus R, et al. Reducing the risk of hallucinations with interpretable deep learning models for low-dose CT denoising: comparative performance analysis. *Phys Med Biol*. 2023;68:19LT01.
36. Liu Z, Li Z, Mhlanga JC, Siegel BA, Jha AK. No-gold-standard evaluation of quantitative imaging methods in the presence of correlated noise. In: *Proceedings of SPIE—the International Society for Optical Engineering*. Vol. 12035. 2022:120350M.
37. Bhardwaj G, Govindarajulu Y, Narayanan S, Kulkarni P, Parmar M. On the notion of hallucinations from the lens of bias and validity in synthetic CXR images. *arXiv preprint*. arXiv:2312.06979; 2023.
38. McCague C, MacKay K, Welsh C, et al. Position statement on clinical evaluation of imaging AI. *Lancet Digit Health*. 2023;5:e400–e402.
39. Park J, Oh K, Han K, Lee YH. Patient-centered radiology reports with generative artificial intelligence: adding value to radiology reporting. *Sci Rep*. 2024;14:13218.
40. Ji Z, Lee N, Frieske R, et al. Survey of hallucination in natural language generation. *ACM Comput Surv*. 2023;55:1–38.
41. Zhou Y, Cui C, Yoon J, et al. Analyzing and mitigating object hallucination in large vision-language models. *arXiv preprint*. arXiv:2310.00754; 2023.
42. Zhou B, Xie H, Liu Q, et al. FedFTN: personalized federated learning with deep feature transformation network for multi-institutional low-count PET denoising. *Med Image Anal*. 2023;90:102993.
43. Liu X, Eslahi SV, Marin T, et al. Cross noise level PET denoising with continuous adversarial domain generalization. *Phys Med Biol*. 2024;69:085001.
44. Liu Q, Tsai YJ, Guo X, et al. Prompt attention convolution net (PAC-Net) for low-count Zr-89 CD8 ImmunoPET denoising. In: *Society of Nuclear Medicine and Molecular Imaging (SNMMI) Annual Meeting*. 2024.
45. Shi Y, Yang T, Chen C, et al. SearchRAG: can search engines be helpful for LLM-based medical question answering? *arXiv preprint*. arXiv:2502.13233; 2025.
46. Antun V, Renna F, Poon C, Adcock B, Hansen AC. On instabilities of deep learning in image reconstruction and the potential costs of AI. *Proc Natl Acad Sci U S A*. 2020;117:30088–95.
47. Yu B, Ozdemir S, Wu J, et al. PET image denoising via text-guided diffusion: integrating anatomical priors through text prompts. *arXiv preprint*. arXiv:2502.21260; 2025.
48. Liu X, Huang Y, Marin T, et al. Dual prompting for diverse count-level PET denoising. In: *Proceedings of the IEEE International Symposium on Biomedical Imaging*. 2025:87–103.
49. Chen T, Hou J, Zhou Y, et al. 2.5D multi-view averaging diffusion model for 3D medical image translation: application to low-count pet reconstruction with CT-less attenuation correction. *IEEE Trans Med Imaging*. 2025.
50. Xia M, Yang H, Qu Y, et al. Multilevel structure-preserved GAN for domain adaptation in intravascular ultrasound analysis. *Med Image Anal*. 2022;82:102614.
51. Budd S, Robinson EC, Kainz B. A survey on active learning and human-in-the-loop deep learning for medical image analysis. *Med Image Anal*. 2021;71:102062.

- 52. Wang Z, Bingham G, Yu AW, Le QV, Luong T, Ghiasi G. Haloquest: a visual hallucination dataset for advancing multi-modal reasoning. In: *Proceedings of the European Conference on Computer Vision*. 2024;288–304.
- 53. Xia M, Ko KY, Wang DS, et al. Anatomically and metabolically informed diffusion for unified denoising and segmentation in low-count PET imaging. *arXiv preprint*. arXiv:2503.13257; 2025.
- 54. Rahman MA, Yu Z, Laforest R, Abbey CK, Siegel BA, Jha AK. DEMIST: a deep-learning-based detection-task-specific denoising approach for myocardial perfusion SPECT. *IEEE Trans Radiat Plasma Med Sci*. 2024.